Communications in Physics, Vol. 35, No. 1 (2025), pp. 87-95

DOI: https://doi.org/10.15625/0868-3166/22079

Dispersion management in organic liquid-cladding photonic crystal fiber based on GeSe₂-As₂Se₃-PbSe chalcogenide for super-continuum application

Hieu Van Le[†],

Faculty of Natural Sciences, Hong Duc University, 565 Quang Trung Street, Thanh Hoa City, Vietnam

E-mail: †levanhieu@hdu.edu.vn

Received 15 December 2024 Accepted for publication 5 February 2025 Published 6 March 2025

Abstract. We present a numerical study of the influence of the liquids on fiber properties. The photonic crystal fiber (PCF) was proposed based on the GeSe₂–As₂Se₃–PbSe chalcogenide, infiltrated with six organic liquids in air holes in the cladding. The guiding properties in terms of dispersion characteristics, mode area, nonlinear coefficient, and confinement loss of the fundamental mode were numerically investigated. The result is that it is possible to shift the wavelength of the zero dispersion by about 20 nm to longer wavelengths, and to reduce the slope of the dispersion curve of the fiber by the liquid filling. The results obtained also show that the PCF has a larger mode area (lower nonlinear coefficient) when infiltrated with liquids with a higher refractive index. At the same time, the presence of liquid in the cladding is responsible for the increase in confinement loss. In particular, the fiber has a lower confinement loss when infiltrated with liquids with a higher refractive index.

Keywords: photonic crystal fiber; dispersion characteristics; chalcogenide, liquids.

Classification numbers: 42.55.Tv; 42.60.Jf; 77.22.Gm.

1. Introduction

Photonic crystal fibers (PCFs) have attracted the attention of researchers in the field of optical communication since it was first fabricated in 1996 [1]. Since the cladding structure of PCF can be flexibly adjusted according to practical applications, it has unique optical properties such as endless single-mode operation over a wider spectrum [2], large birefringence [3], and high nonlinearity [4]. Therefore, optical devices based on PCFs have gradually become a hotspot of research. Recently, PCFs have been applied in the fields of optical communication, nonlinear optics [5], fiber lasers and amplifiers [6], and super-continuum (SC) generation [7].

The controllability of dispersion properties in PCFs is an important issue for practical applications in optical telecommunications, especially for SC light courses. In some nonlinear processes, e.g., four-wave mixing, maintaining phase matching between pulses is the main concern [8,9]. The main cause of phase mismatch in PCFs is the dispersion characteristics, which can significantly affect the efficiency of the nonlinear processes [10,11]. The magnitude of the dispersion properties and even the slope of the dispersion curve have an important impact on the phase matching between pulses over a range of wavelengths [9]. The problem of phase matching in nonlinear processes can be solved by using highly nonlinear PCFs with dispersion properties close to zero. Meanwhile, in SC generation applications, dispersion critically determines the generation of new wavelength components in nonlinear optical fibers during spectrum broadening [12, 13]. Therefore, the dispersion characteristic of the fiber is a crucial criterion in developing nonlinear optical fibers for SC applications.

With PCFs, the dispersion properties can be controlled in a broad spectral range via the lattice constant and the filling factor [14, 15]. For example, an increase in the filling factor, for a certain value of lattice constant leads to a shift of the zero-dispersion wavelength (ZDW) to the shorter wavelengths. Conversely, for a given value of the filling factor, the ZDW is shifted to longer wavelengths and the chromatic dispersion curves shift towards the normal dispersion regime when the lattice constant is increased [14]. The use of different materials opens a new degree of freedom for PCF design. Particularly, by using different materials, it is possible to shift the ZDW and change the dispersion shape [15]. In addition, the dispersion of the PCF can be further modified by infiltrating the air holes with different liquids [16, 17]. Filling the core of a hollow core PCF with a highly nonlinear liquid can significantly increase the nonlinear coefficients due to the high nonlinear refractive index of liquids and the tight mode confinement in PCFs [16].

Furthermore, low dispersion over a wide range can reduce the phase mismatch among interactive optical waves to enhance the high nonlinear conversion efficiency [18]. Therefore, a wide spectral range with low and flat dispersion enables broadband applications such as ultrashort pulse, and wideband optical amplification [19], especially, for SC generation [8]. In our previous works [20], PCF made of GeSe₂–As₂Se₃–PbSe chalcogenide obtained low and ultra-flat dispersion characteristics with fourth ZDWs by changing the diameter of the cladding air holes. However, different diameters of air holes are also a real challenge in manufacturing. To overcome this drawback, in this work, we numerically investigate the optical properties of PCF infiltrated with different liquids. The fiber of GeSe₂–As₂Se₃–PbSe chalcogenide has a hexagonal structure consisting of six air hole rings in the cladding. The selected liquids are highly non-linear, nontoxic, or low-toxic organic solvents. Six organic solvents were considered in this work. The guiding properties in terms of dispersion characteristics, mode area, nonlinear coefficient, and confinement loss of the fundamental mode were investigated numerically.

2. Design of the PCF and theory

In this section, we consider a conventional PCF whose background materials consist of chalcogenide (GeSe₂-As₂Se₃-PbSe), and air-holes in the cladding filled with C₂Cl₄, CCl₄, C₂H₄Br₂, CHCl₃, C₂H₅OH, and C₇H₈. The cross-section of the PCF is shown in Fig. 1. It is assumed that it has six rings with air holes of the same diameter ($d = 1.6 \,\mu$ m), arranged in a hexagonal structure with a lattice constant $\Lambda = 2.0 \,\mu$ m.

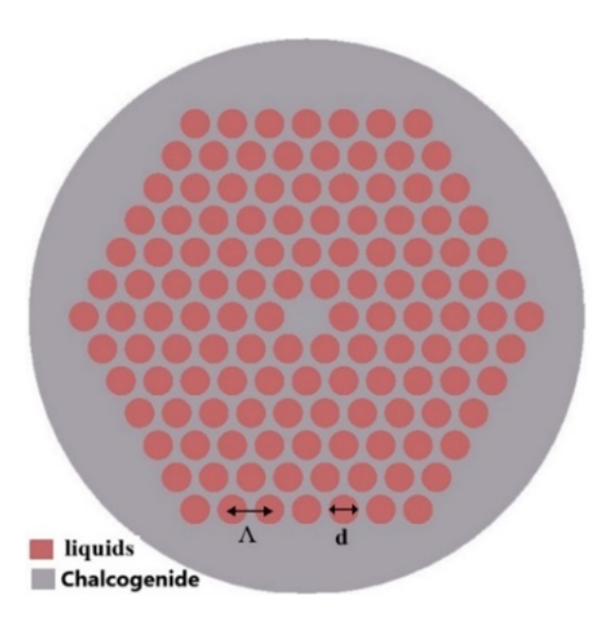


Fig. 1. Cross-sectional structure of the designed PCF.

The Sellmeier equation gives the refractive index dependent on the wavelength of the materials used as below:

$$n = \sqrt{A_0 + \frac{B_1 \lambda^2}{\lambda^2 - C_1} + \frac{B_2 \lambda^2}{\lambda^2 - C_2}}.$$
 (1)

where the constants B_i and C_i (i = 1,2) in the Sellmeier equation for these materials are listed in Table 1. The refractive index of the materials used in this work are shown in Fig. 2. As can be seen in Fig. 2, the refractive index of $GeSe_2-As_2Se_3-PbSe$ is larger than that of the other liquids mentioned. Therefore, the guiding mechanism is provided by total internal reflection along the fiber. Fig. 2(b) shows the transmission spectrum of GAP-Se in the wavelength range from 0 to $10 \, \mu m$. This glass has a wide transparency window, ranging from 1.0 to $20.0 \, \mu m$. The presence of As_2Se_3 component will increase the transparency of this chalcogenide which is much wider than other chalcogenide glasses [21]. Another advantage of GAP-Se chalcogenide is that this glass has a high nonlinear refractive index compared with other glass [16].

The chromatic dispersion is the phenomenon in which the phase velocity of a light wave depends on its frequency. The control of chromatic dispersion in the photonic crystal fiber (PCF) can be achieved by manipulating geometric factors like pitch Λ , diameter d, and the arrangement of air holes within the PCF structure. The dispersion of a PCF is calculated from the $n_{\rm eff}$ using the group-velocity dispersion equation as follows [9]:

$$D = -\frac{\lambda}{c} \frac{d^2 \text{Re}[n_{\text{eff}}]}{d\lambda^2},\tag{2}$$

where c and λ denote the speed of light in a vacuum and the wavelength, respectively. Re[n_{eff}] is the real part of the refractive index.

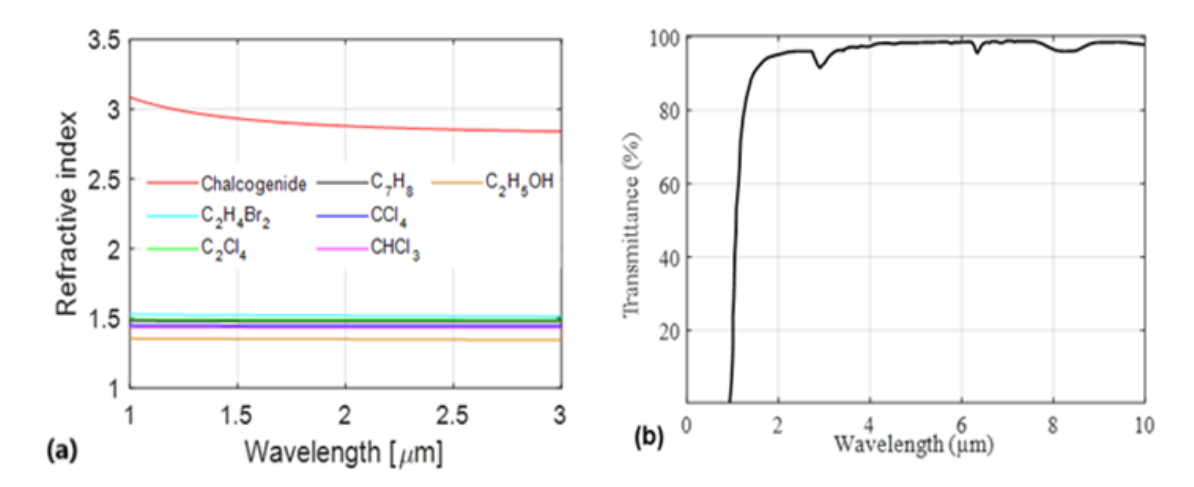


Fig. 2. (Color online) (a) Refractive index of materials used and (b) transmission spectrum of the chalcogenide [21].

Coefficient	A_0	B_1	B_2	$C_1 [\mu \text{m}^2]$	$C_2 [\mu \mathrm{m}^2]$
GeSe ₂ -As ₂ Se ₃ -PbSe [20]	-20.6611	28.5635	10.4782	0.0534534	8175.52
C ₂ Cl ₄ [22]	1	1.21454	0.0350142	0.01456	123.107
CCl ₄ [23]	1	1.09215	0	0.01187	0
$C_2H_4Br_2$ [14]	1	1.31637	0.401322	0.0161612	142.2298902
CHCl ₃ [24]	1	1.04647	0.00345	0.01048	0.15207
C ₂ H ₅ OH [16]	1	0.8318	-0.1558	0.0093	-49.452
C ₇ H ₈ [25]	1	1.17477	0	0.01825	0

Table 1. Sellmeier coefficients of materials used.

One of the most important properties of a strong nonlinear fiber is its nonlinear coefficient. The nonlinear coefficient γ is defined as follows [9]:

$$\gamma(\lambda) = \frac{2\pi n_2}{\lambda A_{\text{eff}}},\tag{3}$$

where n_2 is a nonlinear refractive index and A_{eff} is an effective area of the fundamental fiber mode, defined as [9]:

$$A_{\text{eff}} = \frac{\left(\iint |E|^2 dx dy\right)^2}{\iint |E|^4 dx dy},\tag{4}$$

where E in the formula is the transverse electric field component.

The confinement loss L_c is the ability of light confinement in the core region and is calculated using Eq. (5). Increasing the number of air hole rings supports the confinement of light in the core area and leads to lower losses than in the models with fewer air hole rings. In addition, increasing the air hole radius increases the air-filling factor and reduces the confinement loss

accordingly [9]:

$$L_C = 8.686k \operatorname{Im}[n_{\text{eff}}],$$
 (5)

where k is the wave number ($k = \frac{2\pi}{\lambda}$) in free space, and $\text{Im}[n_{\text{eff}}]$ is the imaginary part of the effective refractive index, and the unit is usually dB/m.

To analyze the fiber's optical properties as a function of the geometrical parameters, the numerical model of the fiber was created. The modes were calculated with a finite-difference eigenmode (FDE) solver. The chromatic dispersion, and confinement loss of the fundamental mode were calculated using the full-vector finite-difference method based on perfectly matched layer boundary conditions using the commercial software Lumerical MODE.

3. Simulation results and discussion

In this section, we consider the optical properties of PCFs when the air holes are filled with liquids in the cladding. The chromatic dispersion of the fundamental mode is calculated as a function of wavelengths in the range of 1.5–5 μ m in Fig. 3. The black lines show the dispersion characteristics in the fiber without liquid. When liquids enter the air holes, the dispersion slope is reduced. For example, at the wavelength of 3.2 μ m, the dispersion value reduces from 38.73 (ps/nm/km) to 0.837 (ps/nm/km), corresponding to the non-infiltrated and infiltrated C₂H₅OH fibers, respectively. At the same time, the ZDW of the fibers is shifted by about 20 nm towards longer wavelengths. The ZDWs of the fundamental mode of the fibers are 3.0, 3.12, 3.16, 3.17, 3.175, 3.178, and 3.20 μ m, for un-infiltrated and C₂H₄Br₂, C₂Cl₄, C₇H₈, CCl₄, CHCl₃, and C₂H₅OH infiltrated fibers, respectively. The results obtained are interesting because the low dispersion near the ZDW ensures the creation of a broad super-continuum with strong confinement at the core.

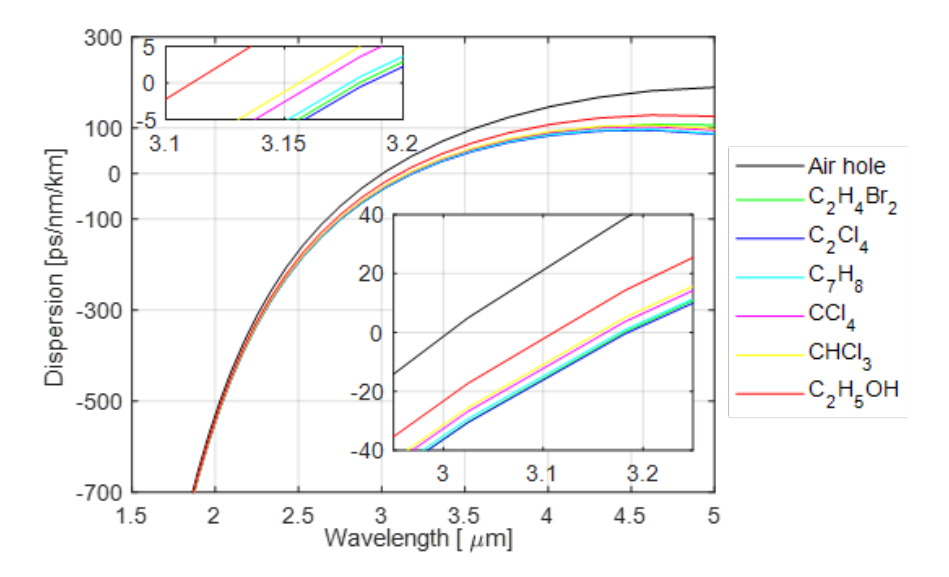


Fig. 3. (Color online) Dispersion of the fiber filled with liquids as a function of the wavelength. The black line denotes the dispersion characteristic obtained in the fiber without liquid.

The numerical values of the effective mode area calculated for the liquid-filled PCF and without liquid are shown in Fig. 4. The comparison shows that the mode area increases when the fiber is filled with a liquid. In particular, the PCF has a larger mode area when it is infiltrated with liquids with a higher refractive index. The smallest increase is observed with ethanol, and the biggest with $C_2H_4Br_2$. For the case of a wavelength of 3.0 μ m, the mode area increases from 3.175 μ m² for air holes to 3.293 μ m² for ethanol, 3.334 μ m² for CHCl₃, 3.34 μ m² for CCl₄, 3.353 μ m² for C_7H_8 , 3.355 μ m² for C_2Cl_4 , and 3.372 μ m² for $C_2H_4Br_2$. The increase in mode area is relatively small, which is advantageous for nonlinear applications.

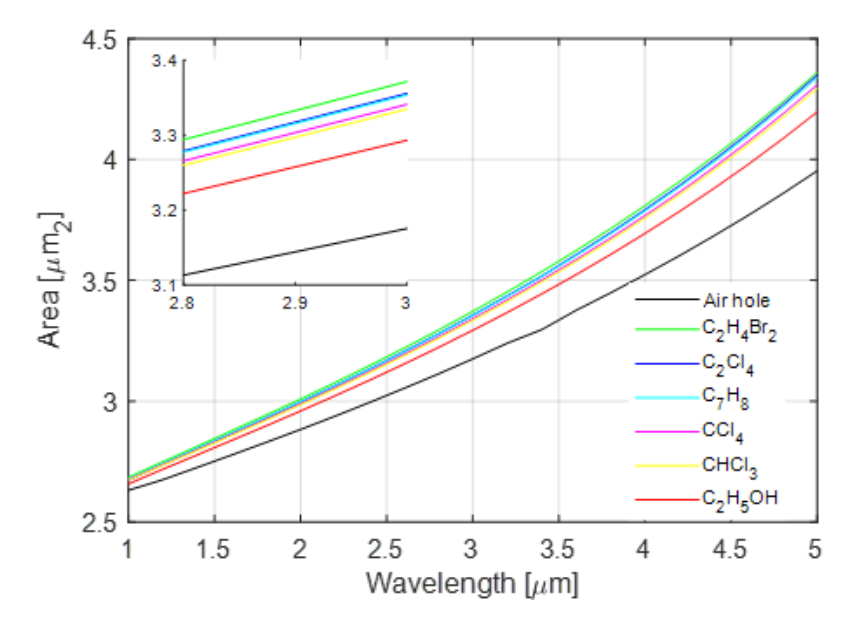


Fig. 4. (Color online) The mode area of the fundamental mode for the fiber-filled-liquids. The black line denotes the fiber without liquid.

The nonlinear parameters related to the mentioned PCF and calculated with equation (3) are also shown in Fig. 5. As can be observed, the nonlinear coefficient for the fiber decreases with increasing wavelength in all cases. The liquid filling of the air hole in the cladding is the cause of the decrease in the nonlinear coefficient of the fiber. At the same time, the fiber has a lower nonlinear coefficient if it is infiltrated by liquids with a higher refractive index.

Lastly, we calculated the fiber confinement loss as a function of wavelength for the liquid-filled fiber. The results are shown in Fig. 6. For all liquid-filled fibers, the confinement loss of the fiber increases. The confinement loss tends to increase with increasing wavelength. In particular, the fiber has a lower confinement loss when it is filled with liquids with a higher refractive index. The highest confinement loss is observed for fibers infiltrated with $C_2H_4Br_2$, and the lowest is for ethanol. For example, at the wavelength of 4.5 μ m, the confinement loss increases from 2.16×10^{-13} dB/m for ethanol to 29.65×10^{-13} dB/m for $C_2H_4Br_2$. Results also show that the confinement loss at a level of 10^{-11} dB/m does not limit the super-continuum generation because the SC generation process can be achieved in a fiber sample only a few centimeters long. In addition, the results have also shown that the fibers exhibit a negative loss at the smaller wavelength

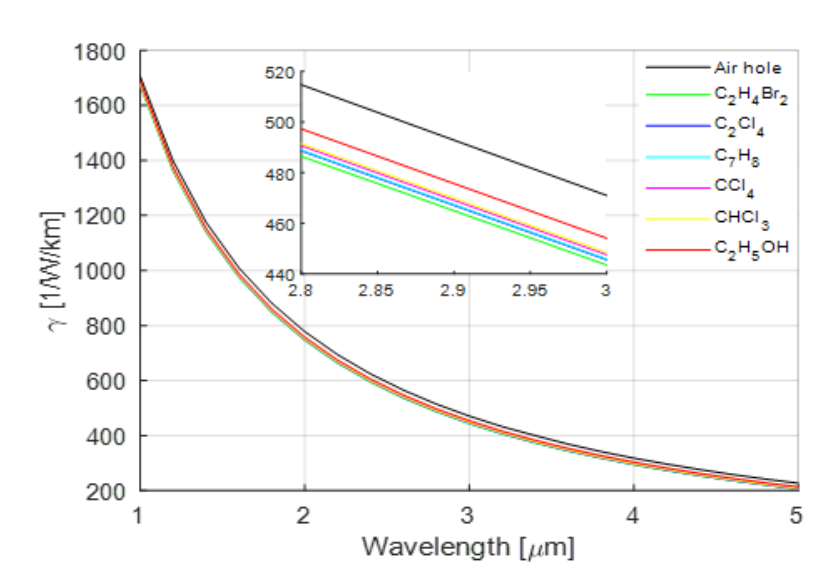


Fig. 5. (Color online) The nonlinear coefficient of the fundamental mode for the fiber-filled-liquids. The black line denotes the γ obtained in the fiber without liquid.

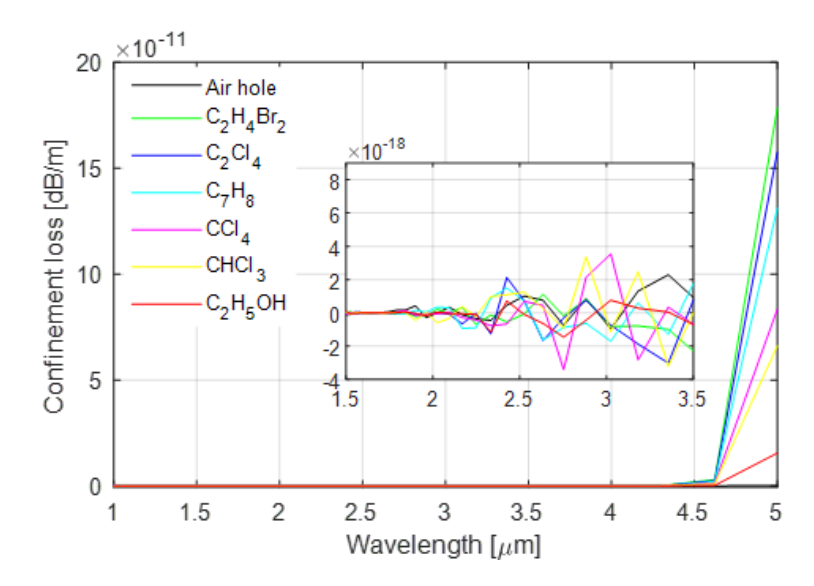


Fig. 6. (Color online) Confinement loss of the fiber as a function of the wavelength for different liquids. The black line denotes the fiber without liquid.

of 4.5 μ m. This is because the fiber is made of GeSe₂–As₂Se₃–PbSe, which has a high nonlinear refractive index, where the amplification of nonlinear effects such as self-phase modulation (SPM) and stimulated Raman scattering (SRS) can lead to reversible losses. This means that energy in the fiber can be "amplified", so that electromagnetic waves can propagate through the fiber without energy loss.

4. Conclusion

In this work, we report a numerical study of the dispersion characteristics of photonic crystal fibers (PCFs) infiltrated with liquids. PCFs were proposed based on the GeSe₂-As₂Se₃-PbSe chalcogenide, infiltrated with six organic liquids in air holes in the cladding. We found that it is possible to control the zero-dispersion wavelength (ZDW) and the shape of the dispersion characteristics of the fiber using liquid filling. When liquids enter the air holes, the dispersion slope is reduced. At a wavelength of 3.2 µm, the dispersion value decreases from 38.73 (ps/nm/km) to 0.837 (ps/nm/km), corresponding to the non-infiltrated and infiltrated C₂H₅OH fibers, respectively. This means that it is possible to use the infiltrated liquids in the cladding of the fiber to reduce the dispersion value (up to 97%). At the same time, the ZDW of the fiber shifts by about 20 nm to longer wavelengths. It can be seen the PCF has a larger mode area when it is infiltrated with liquids with a higher refractive index. The presence of liquid in the cladding is responsible for the increase in confinement loss. In particular, the fiber has a lower confinement loss when it is infiltrated by liquids with a higher refractive index. The results obtained are interesting because the low dispersion near the ZDW gives rise to a broad super-continuum with strong confinement at the core. Moving the ZDW with the liquid-filled approach as desired allows us to use available lasers with femtosecond optical pulses as input sources.

Acknowledgement

This research is funded by Hong Duc University under grant number ĐT-2024-04.

Conflict of interest

The author declare that there are no conflicts of interest.

References

- [1] J. C. Knight, T. A. Birks, P. S. J. Russell and D. M. Atkin, *All-silica single-mode optical fiber with photonic crystal cladding*, Opt. Lett. **21** (1996) 1547.
- [2] M. A. Habib and M. S. Anower, Low loss highly birefringent porous core fiber for single mode terahertz wave guidance, Curr. Opt. Photon. 2 (2018) 215.
- [3] E. Wang, Q. Han, X. Zhou, H. Yuan and J. Li, A bend-resistant photonic crystal fiber with large effective mode area, Opt. Fiber Technol. 71 (2022) 102902.
- [4] R. Saha, M. M. Hossain, M. E. Rahaman and H. S. Mondal, *Design and analysis of high birefringence and nonlinearity with small confinement loss photonic crystal fiber*, Front. Optoelectron. 12 (2019) 165.
- [5] Z. Shen, K. Li, C. Jia and H. Jia, Mid-infrared dual-cladding photonic crystal fiber with high birefringence and high nonlinearity, Optical Review 27 (2020) 296.
- [6] T. Sylvestre, E. Genier, A. N. Ghosh, P. Bowen, G. Genty, J. Troles et al., Recent advances in supercontinuum generation in specialty optical fibers, J. Opt. Soc. Am. B 38 (2021) F90.
- [7] W. J. Wadsworth, A. O. Blanch, J. C. Knight, T. A. Birks, T. P. M. Man and P. S. J. Russell, *Supercontinuum generation in photonic crystal fibers and optical fiber tapers: a novel light source*, J. Opt. Soc. Am. B 19 (2002) 2148.
- [8] J. M. Dudley, G. Genty and S. Coen, Supercontinuum generation in photonic crystal fiber, Rev. Mod. Phys. 78 (2006) 1135.
- [9] G. P. Agrawal, Nonlinear Fiber Optics. Academic Press, Elsevier, 2013, 10.1016/B978-0-12-397023-7.00011-5.
- [10] S. Roy, D. Ghosh, S. K. Bhadra and G. P. Agrawal, Role of dispersion profile in controlling emission of dispersive waves by solitons in supercontinuum generation, Opt. Commun. 283 (2010) 3081.

- [11] I. A. Sukhoivanov, S. O. Iakushev, O. V. Shulika, J. A. A. Lucio, A. Diez and M. Andres, *Supercontinuum generation at 800 nm in all-normal dispersion photonic crystal fiber*, Opt. Express **22** (2014) 30234.
- [12] C. Huang, M. Liao, W. Bi, X. Li, L. Hu, L. Zhang et al., Ultraflat, broadband, and highly coherent supercontinuum generation in all-solid microstructured optical fibers with all-normal dispersion, Photon. Res. 6 (2018) 601.
- [13] Y. Huang, H. Yang, S. Zhao, Y. Mao and S. Chen, Design of photonic crystal fibers with flat dispersion and three zero dispersion wavelengths for coherent supercontinuum generation in both normal and anomalous regions, Results Phys. 23 (2021) 104033.
- [14] H. L. Van, V. T. Hoang, T. L. Canh, Q. H. Dinh, H. T. Nguyen, N. V. T. Minh et al., Silica-based photonic crystal fiber infiltrated with 1,2-dibromoethane for supercontinuum generation, Appl. Opt. 60 (2021) 7268.
- [15] T. S. Saini and R. K. Sinha, Mid-infrared supercontinuum generation in soft-glass specialty optical fibers: A review, Prog. Quantum Electron. 78 (2021) 100342.
- [16] H. V. Le, V. L. Cao, H. T. Nguyen, A. M. Nguyen, R. Buczyński and R. Kasztelanic, Application of ethanol infiltration for ultra-flattened normal dispersion in fused silica photonic crystal fibers, Laser Phys. 28 (2018) 115106.
- [17] J. Pniewski, T. Stefaniuk, H. L. Van, V. C. Long, L. C. Van, R. Kasztelanic et al., Dispersion engineering in nonlinear soft glass photonic crystal fibers infiltrated with liquids, Appl. Opt. 55 (2016) 5033.
- [18] Q. Lin, J. Zhang, P. M. Fauchet and G. P. Agrawal, Ultrabroadband parametric generation and wavelength conversion in silicon waveguides, Opt. Express 14 (2006) 4786.
- [19] Z. Jafari, L. Zhang, A. M. Agarwal, L. C. Kimerling, J. Michel and A. Zarifkar, *Parameter space exploration in dispersion engineering of multilayer silicon waveguides from near-infrared to mid-infrared*, J. Lightwave Technol. 34 (2016) 3696.
- [20] H. V. Le, Coherence evolution of multi-pulse pumped super-continuum in multicomponent gese2-as2se3-pbse chalcogenide photonic crystal fiber with four zero-dispersion wavelengths, J. Opt. Soc. Am. B 41 (2024) 2780.
- [21] T. T. Hong, T. N. Xuan, H. T. Nguyen, V. T. Hoang and H. V. Le, Highly coherent supercontinuum generation in a photonic crystal fiber based on gese2-as2se3-pbse chalcogenide in the mid-infrared region, Appl. Opt. 63 (2024) 5494.
- [22] H. L. Van, V. T. Hoang, H. T. Nguyen, V. C. Long, R. Buczynski and R. Kasztelanic, Supercontinuum generation in photonic crystal fibers infiltrated with tetrachloroethylene, Opt. Quantum Electron. 53 (2021) 02820.
- [23] Q. H. Ding, J. Pniewski, H. L. Van, A. Ramaniuk, V. C. Long, K. Borzycki et al., Optimization of optical properties of photonic crystal fibers infiltrated with carbon tetrachloride for supercontinuum generation with subnanojoule femtosecond pulses, Appl. Opt. 57 (2018) 3738.
- [24] C. V. Lanh, V. T. Hoang, V. C. Long, K. Borzycki, K. D. Xuan, V. T. Quoc et al., Optimization of optical properties of photonic crystal fibers infiltrated with chloroform for supercontinuum generation, Laser Phys. 29 (2019) 075107.
- [25] L. C. Van, A. Anuszkiewicz, A. Ramaniuk, R. Kasztelanic, K. X. Dinh, M. Trippenbach et al., Supercontinuum generation in photonic crystal fibers with core filled with toluene, J. Opt. 19 (2017) 125604.